J. Astrophys. Astr. (2001) **22**, 229–249

Wide-Field Imaging With The Mauritius Radio Telescope.

S. Sachdev[1,2] & N. Udaya Shankar[1,2].

[1] *Raman Research Institute, Sadashivanagar, Bangalore 560080, India*
[2] *Department of Physics, University of Mauritius, Reduit, Mauritius*

Received 2001 August 21 ; accepted 2001 October 16.*

Abstract.

The Mauritius Radio Telescope (MRT) is a Fourier Synthesis T-shaped array operating at 151.5 MHz. The primary objective of the telescope is to produce a sky survey in the declination range $-70°$ to $-10°$. A 512 channel digital complex correlation receiver is used to measure the visibility function. The visibilities have to be measured with four different delay settings to image the entire declination range, keeping the effects of bandwidth decorrelation to less than 20% on the longest baseline. To have a reasonable surveying sensitivity this has to be done in one observation schedule. However the existing correlator system which can measure visibilities with only one presettable delay setting for each integration time, cannot meet this requirement. A recirculator system which enables visibility measurements with four different delay settings in one integration time using the existing correlator has been designed and installed to make the MRT an efficient surveying instrument. This paper describes the recirculator system, and the scheme that we use at MRT to calibrate the visibilities measured with different delay settings. The observations carried out for the full sky survey and a section of the wide field image made using the new system are described in this paper.

Key words:

Radio Telescope - Fourier Synthesis - Bandwidth decorrelation - Bandpass sampling - Single Side band system

1. Introduction

Very few surveys of the southern sky exist at frequencies below 1 GHz, and none which are as deep as the 6C survey of the northern sky (Baldwin *et al* 1985). The Mauritius Radio Telescope (MRT) was built to fill this gap. It is a Fourier

*Although this paper was accepted only on 16 October, we have included it because this issue was delayed due to other reasons.

synthesis instrument operating at 151.5 MHz and is situated in the north-east of Mauritius at a southern latitude of 20°.14. The aim of the survey using the MRT is to contribute to the database of southern sky sources in the declination range $-70° \leq \delta \leq -10°$ covering the entire 24 hours of right ascension, with a resolution of $4' \times 4'.6 \sec(\delta + 20°.14)$ and a point source sensitivity of $\sim$200 mJy(3σ).

The MRT is a $\top$-shaped non-coplanar array consisting of a 2048 m long EW arm and a 880 m long south arm. In the EW arm 1024 fixed helices are arranged in 32 groups and in the south arm 16 trolleys with four helices on each, which move on a rail are used. The primary beams of the helices have a full width at half maximum (FWHM) of 60°, and they are mounted with a tilt of 20° toward the south, i.e., the peak of the primary beam is at $\delta = -40°$. This allows a better coverage of the southern sky including the Galactic plane. The outputs of the EW and the south groups are heterodyned to an intermediate frequency (IF) of 30 MHz in the field, and are brought to the observatory building through coaxial cables. In the observatory, these outputs are further amplified and down-converted to a second IF of 10.1 MHz. These are then quantized to 2-bit 3-levels and sampled at 12 MHz. These are further processed in a 512-channel digital complex correlation receiver to measure the visibility function. The 512 complex visibilities are integrated and recorded at intervals of 1 second. At the end of 24 hours of observation the trolleys are moved to a different position so as to sample the NS baselines with a spacing of 1m and new visibilities are recorded. A minimum of 60 days of observing are needed to obtain the visibilities up to the 880 m spacing. A detailed description of the telescope is to be found in Golap *et al* (1998).

A large part of the back-end including the correlator system was acquired from the Clark Lake Radio Observatory (CLRO) (Erickson *et al* 1982). We adapted and modified the CLRO system for use at the MRT. The modified system was then installed and tested with the rest of the system in Mauritius. In this paper we describe the need for a recirculator system to make MRT an efficient surveying instrument. Section 3 describes its design criteria, the hardware developed and its interface to a computer. The method developed for the calibration of the visibilities measured with four delay settings is described in the section 4. The steps involved in the analysis of the recirculator data and a wide field image with its analysis are described in the section 5.

2. Recirculator System

Although the use of larger bandwidths results in a better sensitivity (for continuum observations) of a telescope, it restricts the field of view of the image if the relative delays between the signals being correlated are not compensated. The loss in sensitivity at the edges of the field is appreciable if delays (τ) are comparable to the inverse of the bandwidth. This effect, known as bandwidth decorrelation, is also referred to by other names like chromatic aberration and fringe washing.

In the MRT the EW group has a narrow primary beam of two degrees in RA.

To obtain interference free observations, we restrict the bandwidth to 1 MHz. This bandwidth does not pose a problem for synthesizing the primary beam in the RA direction. However both the EW and the north-south groups have wide primary beams in declination extending from -70° to -10°. We will, therefore, be concerned with compensating geometric delays for zenith angles along the meridian za_o. The delay can be compensated for a zenith angle along the meridian, $za_o^{'}$, by introducing a delay of $\frac{y_\lambda sin(za_o^{'})}{c}$ where y_λ is the baseline (in wavelengths) along the north-south direction. The correlation response around this point in declination, for a rectangular passband from $\left(\nu_o - \frac{\Delta\nu}{2}\right)$ to $\left(\nu_o + \frac{\Delta\nu}{2}\right)$, is then graded by $sinc(\Delta\nu\Delta\tau)$. $\Delta\tau$ is the uncompensated delay in the direction za_0 given by $\Delta\tau = \frac{y_\lambda}{c}\left(\sin(za_o) - \sin(za_o^{'})\right)$ Thompson *et al* (1986). For a given delay compensation, we will be able to observe only a part of the sky with small decorrelation. This is referred to as the delay zone around the point at which the geometrical delay has been compensated. Our design goal is to image the declination range $-70^{\circ} \leq \delta \leq -10^{\circ}$, using a 1 MHz band keeping the bandwidth decorrelation to less than 20 % even on the longest north-south baseline. This requires visibility measurements with four delay settings.

The existing system measures visibilities with only one delay setting. Thus one has to collect data for different delay zones on separate days. So the number of days required to collect a set of data for survey would increase, thereby reducing the surveying sensitivity[1].

A minimum of 60 days of observing are needed to obtain the visibilities up to the 880 m spacing. We measure the visibilities on a given allocation for about 3 sidereal days to ensure interference free data. It therefore takes 180 days to obtain data for all the baselines. However, during this time the Sun moves through half the sky (12 hours in right ascension) thereby preventing full sky coverage with the 6 month data. We therefore carry out the observations in two rounds. In the second round we observe the same NS baselines after about 6 months interval. This ensures that we have night time observations for all the NS baselines.

Measurement of visibilities with four different delay settings on separate days makes the total time required for acquiring data for the survey to be of the order of four years. This would make the MRT a very inefficient surveying instrument.

Thus there is a need for a system which will allow visibility data to be collected for different delay zones on the same day without degradation in sensitivity. This requires a system which would store the samples for T seconds followed by a correlator system that would measure visibilities with each delay setting in $\frac{T}{N}$ seconds. Such a system wherein the data is sampled and stored at a slower rate and then facilitates the correlator to process data N times faster is called a recirculator. To implement this, a dual-buffer memory system is employed between the sam-

[1] Surveying sensitivity is the minimum flux density detectable in a survey of a particular region when the whole survey is completed in a total time t_s seconds. The sensitivity is expressed in terms of t_s rather than t, the time spent on the measurement in any one particular direction.

pler and the correlator. The data from the sampler is stored at a given rate in one bank while the data from the other bank is read and processed N times faster in the correlator. Figure 1 represents the basic principle of a recirculator system.

3. Design Criteria

The MRT receiver system provides an option of using 3.0 MHz, 1.5 MHz, 1 MHz and 0.15 MHz IF bandwidths. One would generally be interested in using the widest band available for more sensitivity. Higher sensitivity would also improve our calibration because we would be able to use weaker and therefore more number of sources for calibration. However, for wide field imaging the bandwidth decorrelation effect (described in the previous section) becomes more severe. Thus, a larger bandwidth would imply measurements of correlations at a larger number of delays to cover a large field of view.

In this section we discuss the choice of bandwidth used, the sampling frequency employed and the size of memory buffers used, and discuss the specifications and criteria for the design of a data acquisition system.

3.0.1 *Choice of bandwidth*

We begin by determining an appropriate bandwidth for use to maximize surveying sensitivity, given that we intend to map 60° of the sky using a correlator system which can work with clock rates of up to 12 MHz. Furthermore, we start with a design goal of letting the maximum loss due to bandwidth decorrelation to be 20% on the longest baseline.

The surveying sensitivity (Christiansen *et al* 1969), SS_{min}, is defined as:

$$SS_{min} = \sqrt{N_D} f_{os} \frac{\sqrt{2}\, 2k_B(\sqrt{T_{sys_{EW}} T_{sys_{NS}}})}{\sqrt{N_b} A_e \sqrt{\Delta\nu t}} \tag{1}$$

where f_{os} is the degradation factor for a digital correlator, N_D is the number of days required to cover the complete zenith angle range, $T_{sys_{EW}}$ and $T_{sys_{NS}}$ are the system temperatures of EW and NS groups respectively. N_D is given by:

$$N_D \geq int\left(\frac{N_{zn}}{N_{del}}\right) \tag{2}$$

where N_{zn} is the number of delay settings needed to cover the required zenith angle range, N_{del} is the number of delays with which the correlations can be measured using a correlator system that can run up to a maximum frequency of f_{corr}^{max} and *int* denotes the integer part of its argument.

N_{zn} depends on the delay range of interest, τ_{range}, and the maximum allowed decorrelation loss, x_{max}, and may be expressed as

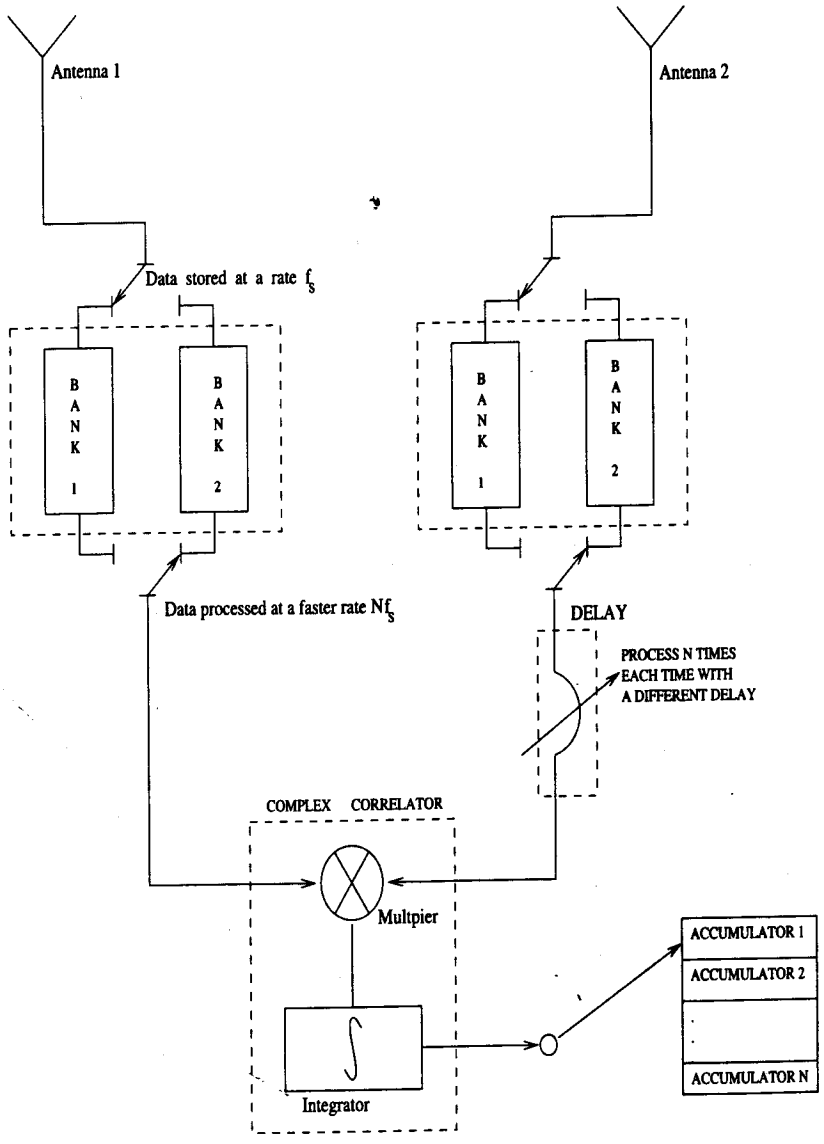

Figure 1. Schematic showing the basic principles of a recirculator. Data is stored at a rate f_s in a dual-buffer memory and is read out and processed at a rate Nf_s in the correlator, allowing data to be processed N times, each time with a different delay compensation.

$$N_{zn} \geq int\left(\frac{\tau_{range}\Delta\nu}{2sinc^{-1}(1-x_{max})}\right) \tag{3}$$

while N_{del} is given by

$$N_{del} \leq int\left(\frac{f_{corr}^{max}}{2\Delta\nu\,\eta}\right) \tag{4}$$

where η is the oversampling factor and $\Delta\nu$ is the bandwidth used.

We therefore note that for a given array, the surveying sensitivity depends upon the following:

(a) the bandwidth used ($\Delta\nu$).

(b) the delay range to be imaged (τ_{range}).

(c) the maximum decorrelation allowed (x_{max}).

(d) the maximum clock speed at which the correlator works (f_{corr}^{max}).

(e) the oversampling factor (η) and the degradation factor f_{os}.

The following have to be considered in obtaining an optimal surveying sensitivity.

(i) The sensitivity obtainable increases as the square-root of the bandwidth. However, the number of days required may increase with the bandwidth. These two factors affect the surveying sensitivity contrarily.

(ii) The sampling frequency has to be set considering

(i) the bandpass sampling criterion.

(ii) that the harmonics of the sampling clock should not fall inside the RF and first IF bands because these can cause spurious correlations.

(iii) The sensitivity also increases to a certain extent with larger oversampling factor for correlators with limited number of bits. However, a larger oversampling factor could reduce the number of delays covered with recirculation for a given correlator speed. This would increase the number of days required, and hence, reduce the surveying sensitivity.

Let us look at items (ii) and (iii) in more detail:

- For a bandpass signal, we need to sample keeping in mind the criterion for bandpass or harmonic sampling.

  The permissible sampling frequencies for a bandpass signal must satisfy the following criterion to avoid loss in sensitivity due to aliasing (Das *et al* 1986).

$$\frac{2}{n}\frac{f_h}{(f_h - f_l)} \leq \frac{f_s}{(f_h - f_l)} \leq \frac{2}{n-1}\left(\frac{f_h}{(f_h - f_l)} - 1\right) \tag{5}$$

where n is an integer such that $1 \leq n \leq \frac{f_h}{f_h - f_l}$, f_h and f_l being the highest and lowest frequencies in the bandpass. In Figure 2 the areas in between a broken line and the next solid line represent permissible sampling regions.

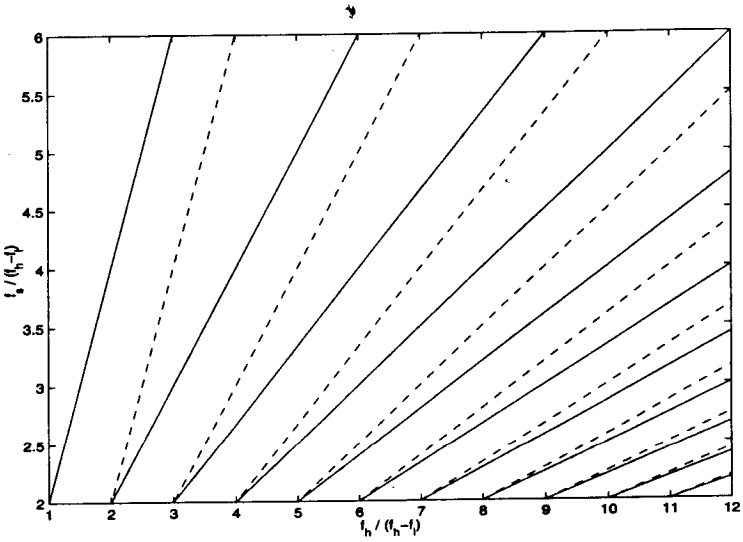

Figure 2. Bandpass sampling criteria: the areas between a broken line and the next solid line represent permissible sampling regions.

- The sampling frequencies that do not have harmonics in the RF (151.5 MHz) and first IF (30 MHz) signal bands.

  The basic system clock may have to be adjusted so that the harmonics of the sampling clock and other clocks used in the system do not fall in the 1 MHz bands about 151.5 MHz and 30 MHz. Harmonic pick-ups on the IF path (30 MHz) which vary faster than the LO switching period would cause spurious correlations and therefore need to be also considered. The duty cycle of the sampling clock also needs to be taken into account because the harmonic contents of the sampling clock depends on it.

- Dependence of sensitivity on the oversampling factor.

  A digital correlator has a lower sensitivity compared to that of an unquantized analog correlator. A band-limited signal that is quantized results in the generation of new frequency components in the waveform, In a digital correlator by sampling at rates higher than the Nyquist rate corresponding to the unquantized waveform, the loss of sensitivity can be reduced.

The dependence of the degradation factor, f_{os}, which is basically the deterioration of sensitivity (Klingler 1972) of a 3 × 3 correlator on the sampling rates is shown in Figure 3.

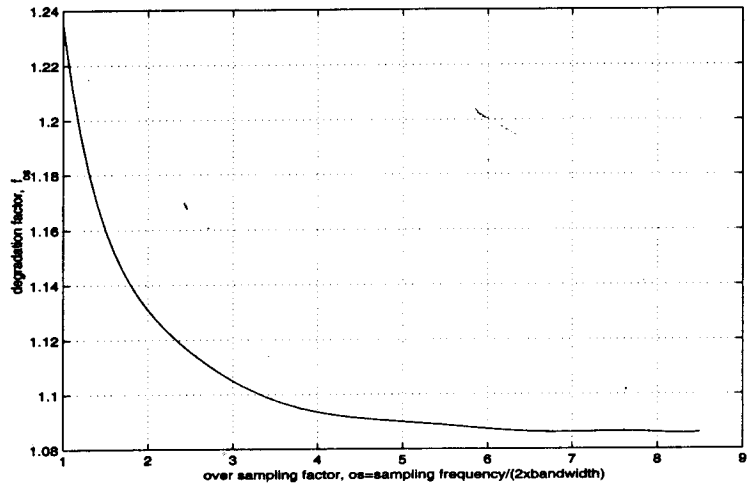

Figure 3. Degradation factor, f_{os}, versus over-sampling factor, η, for a 3 × 3 correlator (Klingler 1972)

We now calculate the surveying sensitivity obtainable with the MRT as a function of bandwidth to cover the full 60° ($-70° \leq \delta \leq -10°$) using a correlator system working at 12 MHz and allowing a maximum decorrelation of 20% on the longest baseline. We normalize the surveying sensitivity with that obtained using a 4 MHz bandwidth which would require 16 days of observations to cover $-70° \leq \delta \leq -10°$ with decorrelation not exceeding 20%. We choose 4 MHz to normalize the surveying sensitivity because this is the maximum bandwidth centered at 10 MHz that we can use with a sampling frequency of 12 MHz. Therefore the normalized surveying sensitivity may be represented as:

$$SS_N = SS_{min} / \left(\frac{1}{1.23} \sqrt{\frac{4 \text{ MHz}}{16 \text{ days}}} \right) \tag{6}$$

where 1.23 is the degradation factor (obtained from Figure 3) for Nyquist sampling in a 3×3 correlator system. The plot of normalized surveying sensitivity is shown in Figure 4.

The plot of surveying sensitivity against bandwidth is not a smooth curve. This is because at some bandwidths the number of days required to cover the entire declination range changes abruptly. From this plot we find that a bandwidth of about 1.1 MHz gives us the best surveying sensitivity. This requires 4 delay settings

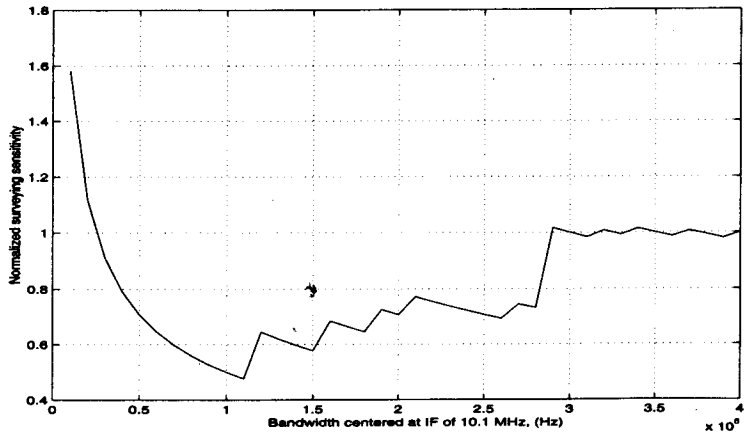

Figure 4. Normalized surveying sensitivity using different bandwidths to image $-70° \leq \delta \leq -10°$ with a 512-channel complex correlator which can work with a maximum clock frequency of 12 MHz.

($N_{del} = 4$), one day ($N_D = 1$) and an oversampling factor of 1.08 ($\eta = 1.08$). The bandwidth which gives surveying sensitivity closest to the above criterion is provided by the 1 MHz filters in the MRT receiver system. So even though the existing system can be used with a 3 MHz bandwidth, for surveying the declination range $-70° \leq \delta \leq -10°$ with the best surveying sensitivity using a 512-channel complex correlator system which can work with a maximum clock frequency of 12 MHz, we use a bandwidth of 1 MHz. This also satisfies our design goal of ensuring that the maximum loss of sensitivity due to bandwidth decorrelation on the longest baseline is 20%. The delay beam of the array which takes into consideration all the interferometers used for imaging will have a lower decorrelation in the different delay zones.

3.0.2 *Choice of sampling frequency*

The plots in Figure 5 show the allowed sampling frequencies according to different criteria for a band of 1 MHz centered at 10 MHz and sampled by a clock with 25% duty cycle, i.e., every fourth harmonic is suppressed. We see in Figure 5(a) the allowed sampling frequency according to the bandpass criterion for a 1 MHz band centered at 10 MHz. Figures 5(b) and 5(c) show the sampling frequencies which do not have harmonics within the 1 MHz band centered at 30 MHz and 151.6 MHz respectively. Figures 5(d) shows the maximum frequency usable to be 3 MHz to allow visibility measurements with four delay settings using a correlator that can work up to a clock frequency of 12 MHz. These different criteria are

finally ANDed to get the permissible sampling frequencies. Figure 5(e) shows the permissible sampling frequencies.

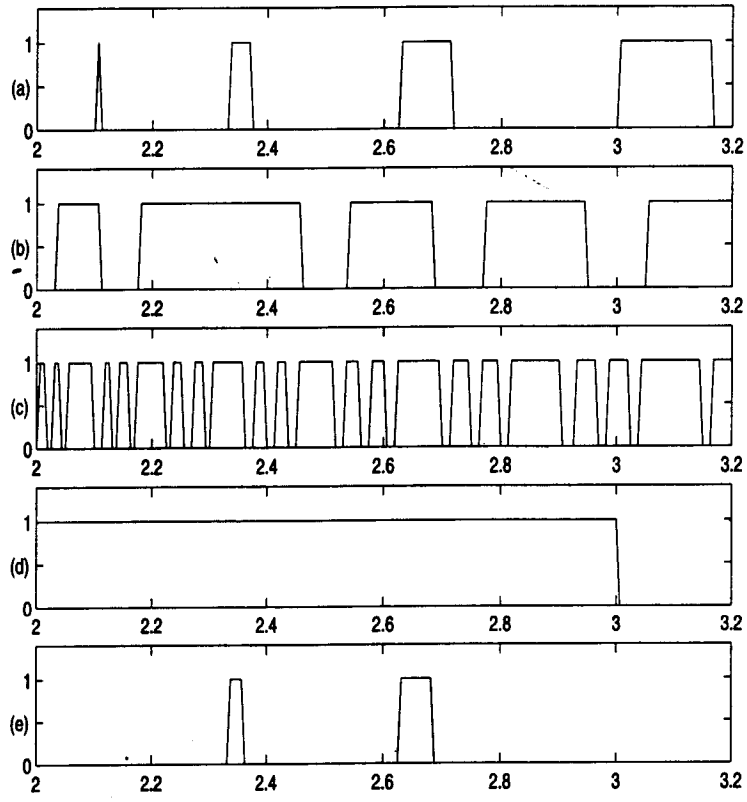

Figure 5. The above plots show the allowed sampling frequencies (a) according to the bandpass criterion for a 1 MHz band centered at 10.1 MHz. (b) which do not have harmonics within the 1 MHz band centered at 30 MHz (c) which do not have harmonics within the 1 MHz band centered at 151.5 MHz (d) for recirculating the data 4 times for the four delay zones using a 12 MHz correlator system (e) obtained after ANDing (a), (b), (c) and (d)

From Figure 5(e), we note that there are two permissible frequency ranges. One extends from 2.3333 MHz to 2.3750 MHz and the other from 2.6250 MHz to 2.7143 MHz. To get better sensitivity we chose a frequency in the higher band, i.e., in the range 2.6250 MHz - 2.7143 MHz. We finally chose a sampling frequency of 2.65625 MHz which is almost at the center of this allowed range of frequencies.

3.0.3 *Choice Of Memory Size*

The size of the memory available on the correlator boards is not enough to take care of the 4 delay zones. Thus it is necessary to transfer the integrated correlation values of each zone to an external memory and then process the other delay zone. The

size of the external RAM would be determined by the integration period required on the correlator boards.

The correlator system at present can output the required 1088 words (512 complex correlations and 64 self-correlations) in about 11 ms ($2^{13} \times 2^4$ clock cycles at 12 MHz $\approx$ 11 ms). For an 11 ms integration period, one needs an external RAM of size 128 K. Thus we undertook the design of a recirculator with external dual memory buffers each of 128 K.

3.1 *Hardware description*

The recirculator system is designed as a modular system consisting of several identical recirculator boards and a central control board for the generation of control signals. The block diagram of a recirculator board is shown in Figure 6.

The recirculator boards have the facility to select :

1. The number of delay zones. These are programmable to 2, 3, or 4 zones. This simultaneously selects the resampling frequency and the integration period.

2. Operation in bypass mode: the data in this mode does not go through the memory of the recirculator.

3. Operation in test mode: In the test mode, test data may be introduced into the recirculator system to test the working of an individual recirculator board. Test data is introduced through the test-buffer on the recirculator boards.

4. Operation in autocorrelation mode: This mode allows the correlator system to be used as a 128 channel auto-correlator directly and with some additional hardware, we can use it as a 4096 channel auto-correlator using the recirculator. The data for the autocorrelation is introduced through the auto-buffer on the recirculator boards.

5. The correlator can be configured in EW and NS fan beam configuration (NS+W)$\times$ NS and (E+W)$\times$E. With the recirculator one can observe in these modes in a time multiplexed mode with (E+W)$\times$S (pencil beam configuration).

3.1.1 *Design criteria for a Data Acquisition System (DAS)*

A PC based design was preferred, since it requires lesser implementation time. At the MRT site, 80386 PCs with ISA bus were readily available. Using a single PC, we were not able to complete all the steps of acquisition such as programming the delays every 11 ms, acquiring the 1088 words of correlation values, integrating them, acquiring the time information from a sidereal clock and then writing to the hard drive once every second. Therefore a data acquisition system employing a dual memory buffer shared by two 80386 PCs running on DOS were used. While one PC acquires and integrates the data onto one bank, the other PC has enough

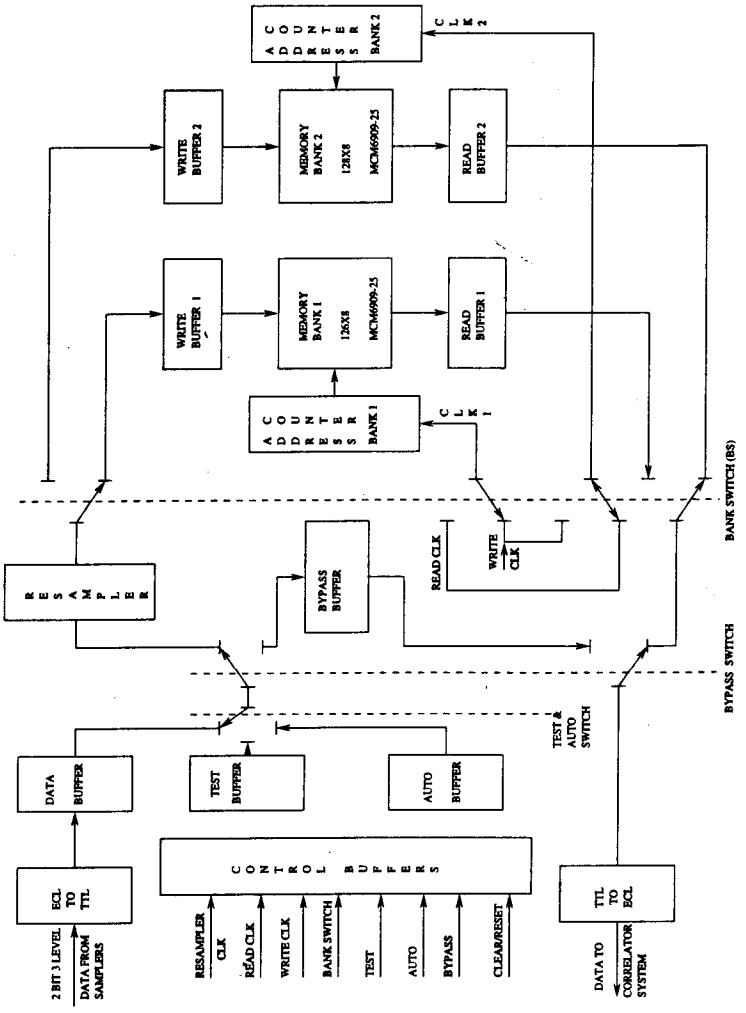

Figure 6. Block diagram of the MRT recirculator board.

time to transfer the data to the hard drive. The block diagram of the control and data acquisition system is shown in Figure 7.

3.2 *System tests*

The system was debugged using static inputs, carrier wave and noise signals as inputs. Finally, data on actual observations of the calibrator source MRC 1932-464 were used to compare the images made using the recirculator data with that

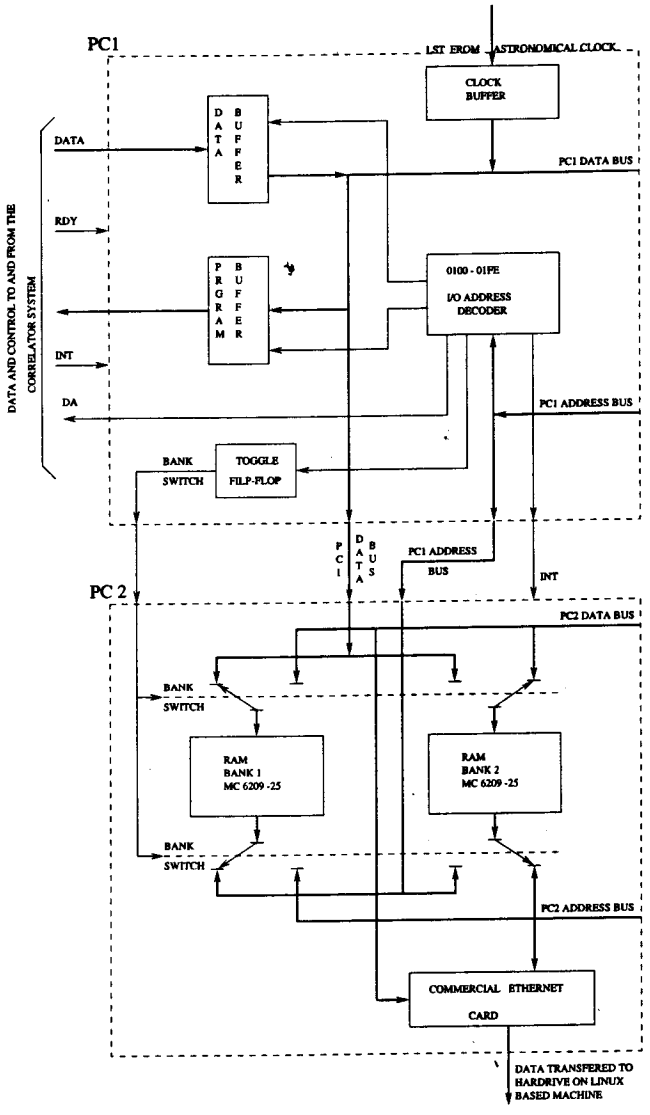

Figure 7. Block diagram of the control and data acquisition system.

obtained without the recirculator. We found the deterioration in the signal-to-noise ratio due to the recirculator to be less than 10%. Since the delays were identical in the two cases, the change in S/N expected was due to the reduced sampling from 12 MHz to 2.65625 MHz. This is of the order of 10%.

These tests and comparisons indicated satisfactory performance of the hardware systems developed.

4. Delay Zone Calibration

The recirculator system was designed to observe with different delay settings. Each delay setting maximizes the correlation in a given range of declination, which is called a delay zone. For imaging different delay zones, one has to calibrate visibilities measured with different delay settings. An ideal calibration scheme would be one in which we use separate calibrators in each declination zone. However we do not have sufficient number of strong calibrators in the southern sky to calibrate the visibilities in the different delay zones. Hence we were forced to use the complex antenna gains estimated for one zone, in which we have a strong calibrator, to calibrate the other zones.

The interferometer setup at MRT is shown in Figure 8. All the relevant equations for this interferometer are also given in this figure. The correlator response $C(\tau)$ of an interferometer obtained by integrating (Fomalont *et al* 1974) the single frequency response over the cross power spectrum may be written as:

$$C(\tau) = \gamma(|\tau_D - \tau|)|G|e^{j(2\pi\overline{\nu_{if}}(\tau_D-\tau)-2\pi(lo_1+lo2)\tau+\phi)} \quad (7)$$

where τ is the geometrical delay, τ_D is the compensating digital delay and $\gamma(|\tau_D - \tau|)$ is the bandwidth decorrelation term (fringe washing term). lo_1 and lo_2 are the first and the second local oscillator frequencies respectively. G is the complex gain of the interferometer expressed in terms of the magnitude $|G|$ and the phase ϕ_{inst}, i.e., $G = |G|e^{j\phi_{inst}}$. $\overline{\nu_{if}}$, is the centroid of the cross power spectrum.

From Equation 7 we see that a discrete change of τ_D produces a phase change equal to $2\pi\overline{\nu_{if}}\tau_D$. This result is used in estimating the complex antenna gains in all delay zones by instrumental calibration of any one of the zones with a strong calibrator.

4.0.1 *Measurement of the cross power spectrum*

We were concerned at the time of the design of the recirculator system about the possibility of unequal IF bandshapes of different antennas leading to variations in the centroids of different interferometers. Such variations limit the accuracy and the sensitivity of the instrument. We carried out measurements of the cross power spectrum of the 512 channels employed for synthesis to calculate the variations in the centroids.

The cross power spectrum is the Fourier transform of the cross correlation function[2]. This was measured using the recirculator system configuring the correlator in the auto/cross correlation mode. The distribution of the 512 band-centroids obtained are shown in Figure 9. It has a mean of 10.1 MHz and an RMS of 0.031 MHz. The measurement of the band-centroids was repeated four times at intervals of about 10 days. No noticeable changes in the band-centroids were seen.

[2]The cross correlation of two waveforms V_1 and V_2 is defined as $\int_{-\infty}^{\infty} V_1(t)V_2^*(t-\tau)dt$

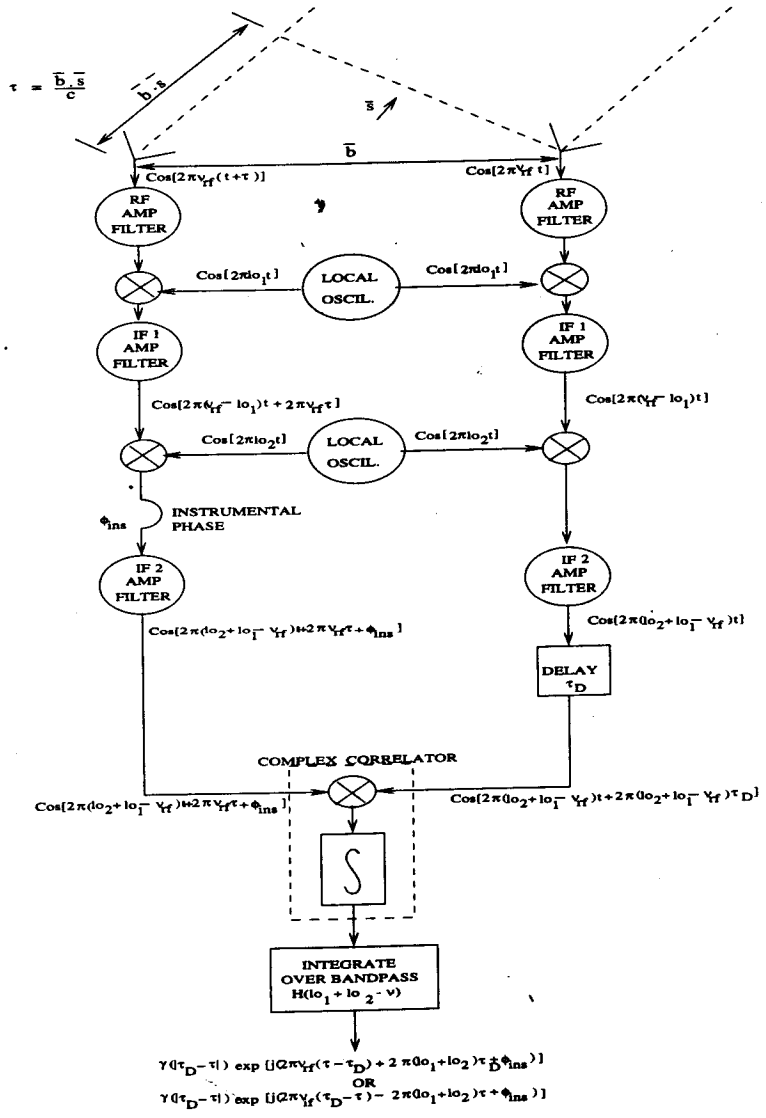

Figure 8. Schematic of the interferometer at the MRT.

The instrumental phase in two delay zones was measured using the calibrator MRC 1932-46 (Flux density $\approx$ 87 Jy) for south baselines less than $\sim$300 m. On these baselines, MRC 1932-46 has a good signal-to-noise ratio in two delay zones. We compared this with the instrumental phase obtained by using the centroid in-

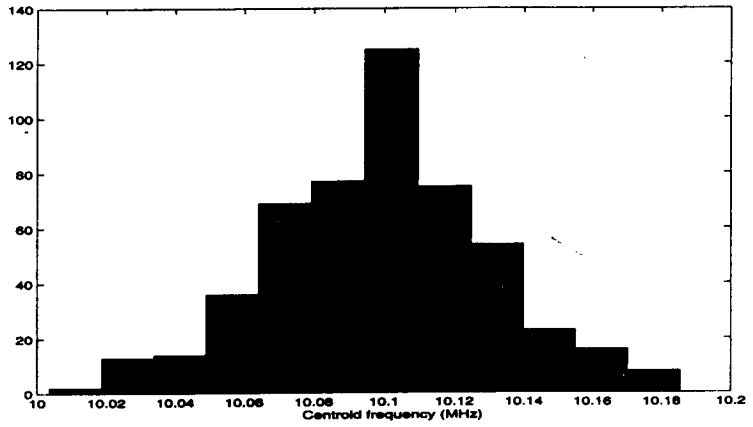

Figure 9. Histogram showing the distribution of the centroids estimated by feeding noise in the laboratory.

formation. A histogram of the difference between the instrumental phases obtained using the two different approaches is shown in Figure 10. The difference has an RMS of 5°. This is expected as the day-to-day phase variations of the instrumental phase estimated using MRC 1932-46 have an RMS of $\sim 10^{\circ}$.

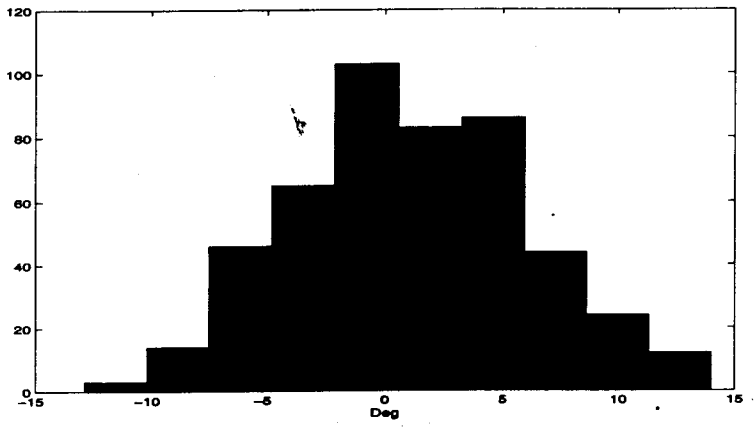

Figure 10. Histogram of difference in phase per delay as derived from the laboratory experiment and that from MRC 1932-46.

There will be phase errors if one uses a value of 10.1 MHz for the band centroids instead of the true values. An RMS variation of 0.031 MHz in the band

centroids leads to an RMS variation in phase of $\theta_1 = 5°$. The day-to-day and source-to-source phase variations are about $\theta_2 = 10°$. The net phase error therefore builds to $\sqrt{\theta_1^2 + \theta_2^2}$=11.18. Thus the spread in the centroid causes the phase errors to increase by only about 10%. The final image is made by combining 32 × 880 visibilities. The dynamic range limitation due to a phase error of 1° ($\frac{1}{1.52}$ radians) will be of the order of $\frac{1}{1.52} \times \frac{1}{\sqrt{32 \times 880}} \approx \frac{1}{850}$. This is quite acceptable. In fact we will be limited in dynamic range mainly due to errors in estimation of the point spread function used to deconvolve the images.

In the future, we plan to improve the calibration using multiple source and redundant baseline calibration techniques. These are expected to reduce phase errors to less than 5°. At that stage one can use the accurate knowledge of the band-centroids. Hence we incorporated the different band-centroid measurements in the calibration program and also in the imaging programs. Unequal bandshapes also limit the use of closure phase in calibration and in deriving antenna based gains from baseline based gains.

5. Wide-field images with a resolution of $4' \times 9'.2 \sec(\delta + 20°.14)$

For making the first wide-field images from the MRT using the recirculator data we chose the region between 19 hrs and 20 hrs in RA. This has the calibrator MRC 1932-464 in the field of view. This choice helped us in the flux density calibration of other sources in the image. Comparison of the estimates of the flux densities and the positional information of these sources with the existing data helps us gain confidence in various tools used for imaging. These images use north-south baselines only up to 441 m, i.e., about the mid-point of the north-south arm.

The flux density of MRC 1932-464 was adapted to be 87 Jy (Golap 1998; Slee 1995) . To obtain the estimates of positions and flux densities of point sources given in the Molongolo Reference Catalog (MRC) (Large *et al* 1981), the expected (theoretical) two-dimensional beam was least-square fitted around the position of the point sources given in the MRC.

A sample image in the right ascension range 19h19m to 19h40m and the declination range $-40°$ to $-29°$ chosen from the data analysed, (Sachdev 1999) is given in Fig.11. Since this is a dirty image, the corrections for the primary beam and for decorrelation have not been applied. 13 MRC sources in the flux density range 3-10 Jy are seen in the image shown. The parameters of the image presented here are summarized in Table 1.

The image is presented in J2000 coordinates. The contour levels are
–1.2, –2.0, –4.0, –6.0, –8.0, –1.5, –2.0, –1.2, –0.8, +0.8, +1.2, +2.0, +4.0, +8.0, +15, +20, +40, +60, +80, +100 Jy/beam.

Observing frequency	151.5 MHz
Minimum and maximum NS baselines	2m, 441m
No of visibilities used per second	$32 \times 440 = 14080$
Right ascension span	19h02m to 19h52m
Declination coverage	$-70°$ to $-10°$
Synthesized beam-width	$4' \times 9'.2 \sec(\delta + 20°.14)$
Point source sensitivity	550 mJy ($1\ \sigma$)

Table 1. Parameters of the images given in this paper.

5.1 *Analysis of the Images*

To estimate the noise in these images, we selected regions which appeared to be devoid of sources. The RMS measured in several such regions were then averaged to get an estimate of the noise. This is about 550 mJy.

We calculated the expected total noise in the image due to contributions from receiver noise, sidelobes of sources, undetected interference and confusion. This is ≈ 450 mJy. We have 20% of the noise which is unaccounted.

We estimated the flux densities and the positions of the sources given in the MRC catalogue. There are 54 sources in the MRC in the RA range 19h02m to 19h52m which are expected (assuming a spectral index of -0.7) to have a flux density $S_{150} \geq 3$ Jy/beam (5σ) in the MRT field of view. Out of these we have been able to detect 53 sources. Only the source MRC 1934-63 was not detected in our image due to its spectral index being different from -0.7. The positional discrepancies in declination are within 2 arcmin. The positional discrepancy in RA is within 0.8 arcmin. We find no systematic errors in position of the declinations and of the right ascensions. We also carried out positional analysis on artificial point sources of various strengths which were added to the images at different places. The errors in these detection were within 1.5 arcmin in declination and 0.7 arcmin in RA. From the ratios of the measured flux to the expected flux densities we have estimated the primary beam of our helix and the delay beam. The deviation from the expected is less than 10% in the declination range of interest.

6. Discussions and Conclusions

During the installation stage of the Mauritius Radio Telescope we identified the need for wide field imaging with this telescope to make it an efficient surveying instrument. We designed and built a recirculator system which allows us to measure visibilities with different delay settings in one observation schedule using the existing correlator. In the recirculator the digitised data is sampled at a rate of 2.65625 MHz, stored in a dual buffer memory and the correlations are measured at four times this rate (10.625 MHz). To program the correlator system and the recirculator boards, and also to acquire data from the correlators, we designed and

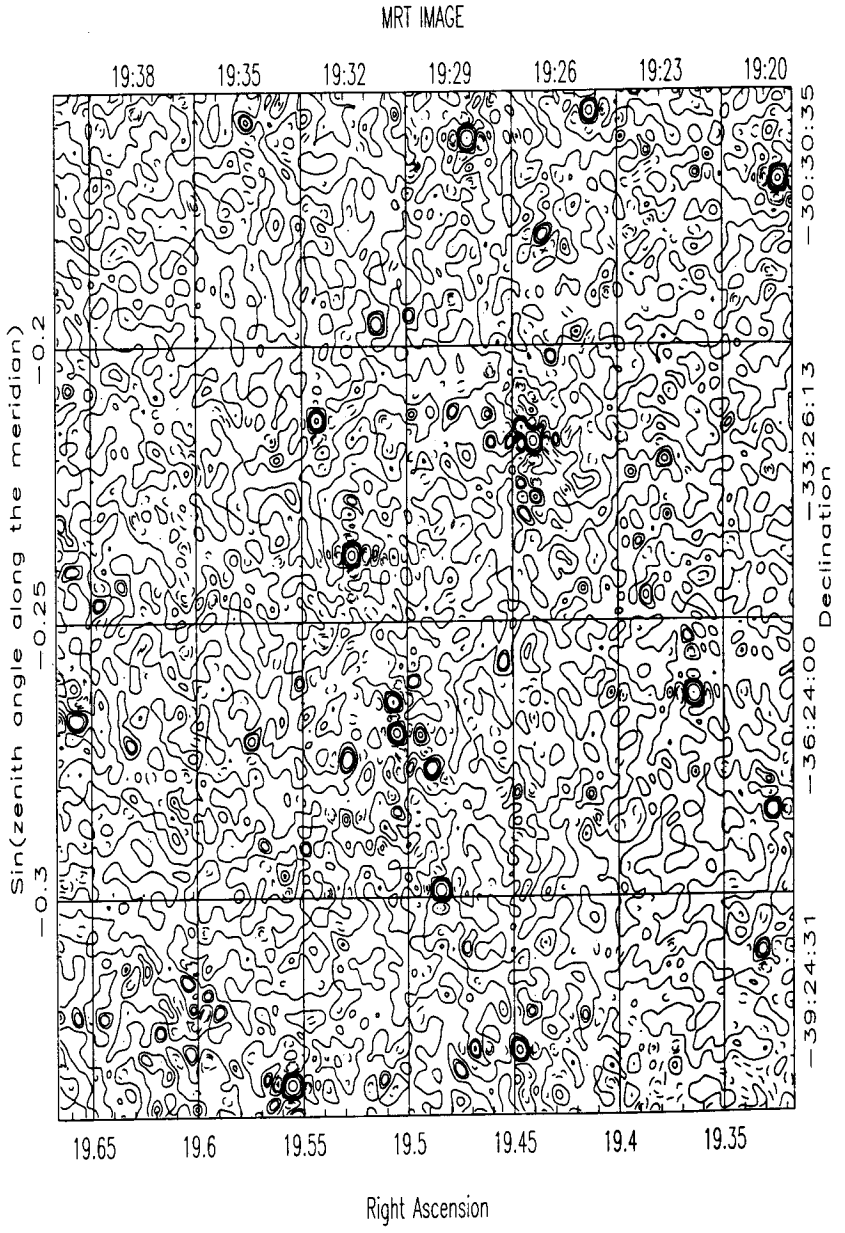

Figure 11. Image in the right ascension range 19h19m to 19h40m and declination range −40° to −29°.

built a new data acquisition and control system (DAS). This data acquisition system comprises of a double bank of memories shared by two PCs running on DOS.

The recirculator system has been integrated into the receiver system at the MRT and tested. After ensuring satisfactory performance, we carried out observations for the survey using the recirculator system up to the longest north-south baseline, i.e., up to 880 m during the period September 1995 to October 1996.

The choice of the usable bandwidth and the sampling frequency for the recirculator has optimised the telescope performance. The methodology described here will also be useful in the design of modern receiver systems where digitisation very early in the receiver chain is preferred. The design has enabled us to measure visibilities with four delay settings, with the existing correlator with only a 10% loss in sensitivity. The hardware has added new features to the existing receiver system. The correlator system can now measure autocorrelation and cross correlation functions up to 128 clock delays. Using the recirculator in this mode the cross power spectrum of the 512 baselines was measured to establish the centroids of their bandpasses. The telescope can also be operated in a time multiplexed mode to measure EW X E and NS X NS baselines. This is useful in the calibration of the array using the Redundant Baseline Calibration technique. The second round of observations for the survey has been carried out in this mode, using $\approx 10\%$ of the observing time to obtain these correlations. With this many strong extended sources can be used for the array calibration and will help to improve the calibration of the visibilities.

Due to paucity of strong sources we have not been able to calibrate the visibilities measured with different delay settings. Using the receiver configuration we have devised a method of estimating the instrumental phase in the four delay zones using a calibrator in only one of the delay zones. This needs information about the centroids of the bandpass used. We measured the variation in the centroids of the bandpasses of the 512 baselines used for imaging and established that variation causes only a 5 degree RMS error in the instrumental phase calibration. Thus the hardware at MRT allows high dynamic range imaging (≈ 1000).

A one hour region around the calibrator MRC 1932-464 with the full declination range of the MRT has been imaged with a resolution of $4' \times 9'.2 \sec(\delta + 20°.14)$. We have carried out some preliminary analysis of these images. The noise in our image is approximately 550 mJy and is only 20% higher than expected. We estimated the position and flux densities of the MRC sources in our image. We have been able to detect in the MRT image, all the 53 sources listed in the MRC catalog in the RA range 19h02m to 19h52m (J2000 coordinates) which are expected to have a flux density $S_{150} \geq 3$ Jy/beam (5σ) in the MRT field of view. The positional discrepancies in declination and in RA are well within the limits expected. We have also detected a number of sources which are not listed in the MRC. A detailed study of these sources will be undertaken in the future and will be published separately. We have thus demonstrated the wide-field imaging capability of MRT using the recirculator system. The usefulness of the recirculator in carrying out a survey with the MRT cannot be over-emphasized.

7. Acknowledgments

The MRT is operated jointly by the Raman Research Institute, Bangalore; Indian Institute of Astrophysics, Bangalore and the University of Mauritius. We thank K. Golap, University of Mauritius and R. Dodson, University of Durham for innumerable discussions during the design and installation of the recirculator; H. A. Ashwathappa, RRI, for his help in carrying out observations. We thank A. A. Deshpande, RRI, for many discussions regarding the design criteria of the recirculator. We thank K. S. Dwarakanath, RRI and Ch. V. Sastry for their valuable feedback on the manuscript. We would also like to thank V.N. Pandey and N. Oozeer for their help in preparing the manuscript.

References

Baldwin, J. E., Boysen, R. C., Hales, S. E. G., Jennings, J. E., Waggett, P. C., Warner, P. J., and Wilson, D. M. A., 1985, *MNRAS*, **217**,717.

Christiansen, W. N., and Hogbom, J. A., *"Radiotelescopes"*. Cambridge university press, 1969.

Das, J., Mullick, S. K., and Chatterjee, P. K., *"Principle of Digital Communication"*. Wiley Eastern Ltd., 1986.

Erickson, W. C., Mahoney, M. J., and Erb, K., 1982, *ApJS*, **50**,403.

Fomalont, E. B., Wright, M. C. H., in *"Galactic and Extragalactic Radio Astronomy"*, Ed. Vrshuur, G.L., Kellermann, K.I., Springer-Verlag, NY, 1974.

Golap, K., *"Synthesis Imaging at 151.5 MHz using the Mauritius Radio Telescope"*. PhD thesis, University of Mauritius, 1998.

Golap, K., Udaya Shankar, N., Sachdev, S., Dodson, R., Sastry, Ch. V., 1998, *J. Astrophys. Astr.*,**19**, 35.

Klingler, R. J. "Quantization noise of signal correlators". Master's thesis, University of British Columbia, 1972.

Large, M. I., Mills, B. Y., Little, A. G., Crawford, D. F., and Sutton, J. M., 1981, *MNRAS*, **194**,693.

Sachdev, S., *"Wide field Imaging with the Mauritius Radio Telescope"*. PhD thesis, University of Mauritius, 1999.

Slee, O. B., 1995, *AuJPh*, **48**,143.

Thompson, A. R., Moran, J. M. and Swenson, G. W. Jr. *"Interferometry and Synthesis in Radio Astronomy"*. John Wiley and Sons, 1986.